THE ASTROPHYSICAL JOURNAL, 288:43–49, 1985 January 1

COUNTERIMAGES IN CLOSED ELLIPTICAL FRIEDMANN UNIVERSES

J. V. NARLIKAR[1]
Kitt Peak National Observatory, National Optical Astronomy Observatories[2]
AND
T. R. SESHADRI
Tata Institute of Fundamental Research, Bombay, India
Received 1984 June 19; accepted 1984 July 23

ABSTRACT

It is shown that the different connectivity implied by the elliptical version of a closed Friedmann model allows two images of a distant astronomical object to be seen, provided the deceleration parameter q_0 of the Friedmann model exceeds unity. Of the two images the "direct image" is along the shortest route light track. If the redshift of the direct image exceeds $(1.5\ q_0 - 1)(q_0 - 1)^{-2}$ then a second "counterimage" should be visible at the diametrically antipodal position. The direct image has a maximum possible redshift $z_{\max}(q_0)$, and it is suggested that the apparent cutoff in the redshifts of QSOs may be due to this effect. Other observable consequences of this result are discussed in relation to galaxies and QSOs.

Subject headings: cosmology — quasars — relativity

I. INTRODUCTION

It is well known that Weyl's postulate and the cosmological principle determine the geometry of spacetime as that given by the Robertson-Walker line element

$$ds^2 = c^2dt^2 - S^2(t)\left[\frac{dr^2}{1 - kr^2} + r^2(d\theta^2 + \sin^2\theta d\phi^2)\right]. \tag{1}$$

Here c = speed of light, t = cosmic time, and (r, θ, ϕ) are the constant spatial coordinates of a typical fundamental observer. The above two assumptions do not determine the scale factor $S(t)$ and the curvature parameter k which takes one of the three possible values $0, \pm 1$. Dynamical considerations, e.g., Einstein's field equations, are expected to determine these unknown quantities.

However, even when the line element (1) is completely known, the topological question of global connectivity is still left unsettled. For example, this line element tells us how to compute the proper separation between two spacetime events whose coordinates differ by infinitesimal quantities; but it does not tell us whether events with finitely separated coordinates are really far apart or even distinct. A two-dimensional example will illustrate this issue. The line element

$$dl^2 = dx^2 + dy^2 \tag{2}$$

describes Euclidean geometry on a plane. However, the substitution $y = a\theta$ changes expression (2) to

$$dl^2 = dx^2 + a^2d\theta^2\ . \tag{3}$$

In this form expression (3) is the familiar line element on a circular cylinder of radius a. The difference between the plane and the cylinder lies in the identification of points whose θ-values differ by multiples of 2π.

In the cosmological case (1) a particularly interesting situation arises for $k = 1$ that corresponds to a closed universe. The spatial section (t = constant) of this spacetime is the hypersurface of a 4-sphere. If the entire hypersurface is covered, then the space is called "spherical," and this is the sense in which the $k = 1$ case is usually interpreted. However, the space can have a different connectivity if the antipodal points of the sphere are identified. The space is then called "elliptical."

Although this distinction had been highlighted in early works on cosmology (see, for example, Eddington, 1923), it appears to have been largely ignored in later works, probably because no astronomical tests for distinguishing between the two versions of the closed universe were available. The purpose of this paper is to discuss ways in which the difference of connectivity could be tested by viable astronomical observations. The rapid improvement in the astronomy of very faint objects and the promises held out by the Space Telescope make such studies not only possible but relevant.

In § II we show that one major difference between the spherical and elliptical spaces is that, under certain circumstances, the latter (but not the former) permits two images of an astronomical object to be seen. The "direct" and brighter image is located in the direction from where the light ray traveling along the shortest route reaches the observer. The second, "counterimage" is fainter and located in a diametrically opposite direction. In § III we will discuss how this result could be used in astronomical observations to distinguish between the spherical and elliptical spaces.

[1] On leave of absence from the Tata Institute of Fundamental Research, Bombay.
[2] Operated by the Association of Universities for Research in Astronomy, Inc., under contract with the National Science Foundation.

Throughout this work we will deal with closed Friedmann models which are obtained as solutions of Einstein's equations with $\lambda = 0$ for dustlike matter. In this context it is important to emphasize that the counterimages considered here are different from the "ghost images" discussed by Petrosian, Salpeter, and Szekeres (1967) in closed spherical models with $\lambda \neq 0$. We will highlight this distinction at an appropriate place in this paper.

II. WHEN ARE TWO IMAGES OBSERVABLE?

To answer the above question it is necessary to take into account the dynamics of the expanding universe. We denote by t_0 the present epoch of observation and use the suffix 0 to indicate values of the various physical quantities at $t = t_0$. Following the usual convention we describe the dynamics of expansion with the help of the Hubble constant and the deceleration parameter:

$$H_0 = \frac{\dot{S}}{S}\bigg|_{t=t_0}, \qquad q_0 = -H_0^{-2} \cdot \frac{\ddot{S}}{S}\bigg|_{t=t_0}. \tag{4}$$

(The overhead dot denotes differentiation with respect to t.)

It is convenient to express t and S as functions of a parameter ψ. For the $k = 1$ case we have

$$t = \frac{\alpha}{c}(\psi - \sin\psi), \qquad S = \alpha(1 - \cos\psi), \tag{5}$$

where

$$\alpha = \frac{c}{H_0} \times \frac{q_0}{(2q_0 - 1)^{3/2}}. \tag{6}$$

Also, the present values are given by

$$S_0 = \frac{c}{H_0}(2q_0 - 1)^{-1/2}, \tag{7}$$

$$\psi_0 = \cos^{-1}\frac{1 - q_0}{q_0}, \tag{8}$$

$$t_0 = \frac{q_0}{(2q_0 - 1)^{3/2}}\left[\cos^{-1}\frac{1 - q_0}{q_0} - \frac{(2q_0 - 1)^{1/2}}{q_0}\right]H_0^{-1}. \tag{9}$$

For details see Narlikar (1983).

a) *The Direct Image*

Consider the ray of light from an emitter at $r = r_e$, leaving it at $t = t_e$ and reaching the observer at $r = 0$ at the present epoch. With the above notation it can be shown that

$$r_e = \sin(\psi_0 - \psi_e), \tag{10}$$

and the redshift of the object is given by

$$z = \frac{q_0(1 + \cos\psi_e) - 1}{q_0(1 - \cos\psi_e)}. \tag{11}$$

ψ_e is related to t_e through expressions (5). The particle horizon at the present epoch is given by setting $\psi_e = 0$ in equation (10):

$$r_H = \sin\psi_0 = \frac{(2q_0 - 1)^{1/2}}{q_0}. \tag{12}$$

b) *The Counterimage*

We now investigate the circumstances under which the counterimage could be seen. To make the distinction between the spherical and elliptical spaces more apparent consider the Euclidean 4-sphere given by

$$x_1^2 + x_2^2 + x_3^2 + x_4^2 = S^2. \tag{13}$$

Since we are considering the t = constant sections of expression (1), S is a constant. Define angular coordinates (χ, θ, ϕ) on the hypersurface (13), by the relations

$$x_1 = S\cos\chi, \qquad x_2 = S\sin\chi\cos\theta, \qquad x_3 = S\sin\chi\sin\theta\cos\phi, \qquad x_4 = S\sin\theta\sin\chi\sin\phi. \tag{14}$$

The complete hypersurface is covered by the coordinate ranges

$$0 \leq \chi \leq \pi, \qquad 0 \leq \theta \leq \pi, \qquad 0 \leq \phi < 2\pi. \tag{15}$$

Since the hypersurface is embedded in a four-dimensional Euclidean space its line element is given by

$$dl^2 = dx_1^2 + dx_2^2 + dx_3^2 + dx_4^2$$
$$= S^2[d\chi^2 + \sin^2\chi(d\theta^2 + \sin^2\theta d\phi^2)] . \quad (16)$$

It is easy to verify that the transformation

$$r = \sin\chi \quad (17)$$

takes expression (16) to the spacelike part of expression (1) with $k = 1$.

Figure 1 illustrates the difference between the spherical space and the elliptical space. It shows a typical great circle of the 4-sphere given by expression (13), containing the observer O at $\chi = 0, r = 0$. In the spherical space, all points in the coordinate ranges (15) are distinct. Thus on the great circle of Figure 1, χ runs through on the left, from $\chi = 0$ through $\chi = \pi/2$ to $\chi = \pi$ as r increases to 1 and decreases back to 0, while $\theta = \theta_0, \phi = \phi_0$ are constants. The right half of the great circle has $\theta = \theta_0, \phi = \phi_0 + \pi \pmod{2\pi}$ as χ runs from 0 to π. The point O′ where $\chi = \pi$ on this circle is antipodal to O, and has the same r value ($r = 0$).

From expression (10) we see that the emitter has to be located at the point E where the arc OE corresponds to $\chi = \chi_e$ given by

$$\chi_e = \psi_0 - \psi_e . \quad (18)$$

Similarly, the particle horizon is indicated on Figure 1 by points H_1, H_2, where the arcs OH_1, OH_2 equal the angle

$$\chi_H = \psi_0 . \quad (19)$$

For a finite $q_0(< \infty)$, $\chi_H < \pi$. This explains why no counterimage can be seen by O in the closed spherical universe. For, to form the counterimage the light ray from E must describe the arc $EH_1O'H_2O$. Since this arc crosses the particle horizon, this ray cannot reach O. In other words, the universe has not been in existence long enough to form the counterimage.

The situation can be different in the elliptical space. Here the connectivity is defined by the identification

$$(x_1, x_2, x_3, x_4) \equiv (-x_1, -x_2, -x_3, -x_4) , \quad (20)$$

i.e., by identifying every point on the hypersurface of the 4-sphere with its antipodal point. In terms of Figure 1 and the coordinate transformation (14), this implies the identification

$$[\chi, \theta, \phi] \equiv [\pi - \chi, \pi - \theta, \pi + \phi \pmod{2\pi}] . \quad (21)$$

Thus the emitter E at χ_e is identified with the diametrically opposite point E′ where the angle subtended by the arc E′O at the center is $\pi - \chi_e$.

In other words, corresponding to the direct image formed along the arc EO, a counterimage along the arc E′O is also possible. As drawn in Figure 1, $\chi_e < \pi/2$ while $\chi_e' \equiv \pi - \chi_e > \pi/2$. (Except in § IIIc, we will assume without loss of generality that $\chi_e' > \chi_e$.) However, for the counterimage to be visible the point E′ must lie closer to O than H_2. If this did not happen, the particle horizon would not permit the second image to be seen. The required condition for a counterimage to be seen is therefore $\chi_e' \leq \chi_H$, i.e., from expressions (18) and (21),

$$\psi_0 \geq \frac{\pi}{2} + \frac{\psi_e}{2} > \frac{\pi}{2} . \quad (22)$$

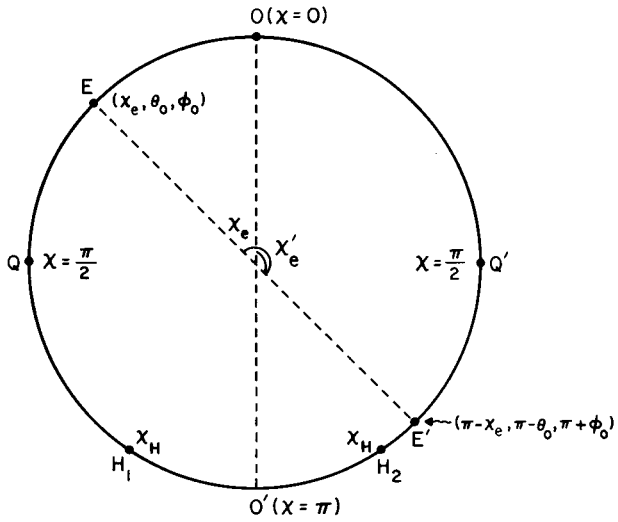

FIG. 1.—A typical great circle on the hypersurface of the 4-sphere which contains the three-dimensional space of the universe at any given time. (O, O′), (Q, Q′), and (E, E′) are pairs of antipodal points. The observer is at O, and H_1, H_2 represent the particle horizon for O.

With the help of expression (8) this last inequality translates to

$$q_0 > 1 \,. \tag{23}$$

Thus, provided the deceleration parameter satisfies the above condition, a counterimage in the opposite direction can be seen in the closed elliptical model.

The counterimage discussed here is different from the ghost images described by Petrosian, Salpeter, and Szekeres (1967) in the following way. The ghost images are supposed to form at the antipodal point in a closed *spherical* universe by the focusing of light rays from the original source. In order that such ghost images would form and be seen by the observer the universe has to have sufficiently long age. Petrosian, Salpeter, and Szekeres (1967) were able to obtain such conditions by choosing a nonzero λ close enough but greater than the critical value λ_c needed to give a static Einstein universe. In our case the counterimage is not a ghost image but involves seeing the real object via the antipodal route in the elliptical universe with $\lambda = 0$, $q_0 > 1$.

III. OBSERVABLE CONSEQUENCES

a) Redshift Pairs

A direct observable consequence of the above result is that provided we live in a closed elliptical universe with $q_0 > 1$, an object seen via the direct route with a redshift exceeding a minimum value $z_{\min}(q_0)$ would have a counter image in exactly the opposite direction with larger redshift.

$z_{\min}(q_0)$ is obtained from inequality (22) by taking the equality, i.e., by letting E′ in Figure 1 coincide with H_2. This gives

$$\psi_e = 2\psi_0 - \pi \,, \tag{24}$$

and using equation (11), a simple manipulation gives

$$z_{\min}(q_0) = \frac{3q_0 - 2}{2(1 - q_0)^2} \,. \tag{25}$$

If the direct image has the above redshift, the counterimage would have infinite redshift. As the direct image redshift z increases above $z_{\min}(q_0)$, the counterimage redshift z' decreases from infinity. The two become equal at the redshift

$$z = z' = \frac{q_0 + (2q_0 - 1)^{1/2} - 1}{q_0 - (2q_0 - 1)^{1/2}} \equiv z_{\max}(q_0) \,. \tag{26}$$

This happens when, in Figure 1, the emitter E is located at Q, $\chi_e = \pi/2$, and hence has $\psi_e = \psi_0 - \pi/2$. Thus the redshift range for objects with counterimages is

$$\frac{3q_0 - 2}{2(1 - q_0)^2} < z < \frac{q_0 + (2q_0 - 1)^{1/2} - 1}{q_0 - (2q_0 - 1)^{1/2}} \,. \tag{27}$$

The actual relationship between z' and z for any $q_0 > 1$ is given by the formula

$$z' = \frac{2(q_0 - 1)^3 + q_0(3q_0 - 2)z + 2(q_0 - 1)(2q_0 - 1)(1 + 2q_0 z)^{1/2}}{5{q_0}^2 - 6q_0 + 2 + 2q_0(q_0 - 1)^2 z - 2(q_0 - 1)(2q_0 - 1)(1 + 2q_0 z)^{1/2}} \,. \tag{28}$$

This relationship is illustrated in a series of curves in Figure 2. Notice that the upper limit on z in expression (27) is also the lower limit on z'. For $q_0 = 3$, this value is 5.545 while $z_{\min} = 0.875$. Thus objects in the redshift range (0.875–5.545) are expected to have counterimages, some of them with redshifts as low as $z' \approx 6$. A redshift of 6 will take the Lyman-α line in a quasi-stellar spectrum to the near-infrared. For even higher redshifts it may be necessary to look for lines with even lower rest wavelengths. For example, He II (helium Lyman-α) line has not been hitherto looked for in the quasi-stellar spectra. With a rest wavelength of 304 Å it could be detected below 10000 Å at redshifts $z' \lesssim 30$.

b) Apparent Magnitudes

How much fainter will the counterimages appear compared to the direct image? This question is hard to answer in clear terms for the following reasons.

(i) Light forming the counterimage left the emitter at an epoch earlier than the light which forms the direct image. We do not know how the absolute luminosity of the emitter changed in between the two epochs.

(ii) Because of the large redshifts the K-corrections are very uncertain.

(iii) The light tracks encounter different intervening absorption en route.

As an extreme example of (i), if it is assumed that no galaxies or quasi-stellar objects existed prior to the redshift of ~ 4, say, then, unless $q_0 \gtrsim 4.24$, no counterimage will be seen. The K-corrections can be estimated with some confidence only after the emission continuum in the high-frequency end of the UV spectrum of nearby objects becomes well known, although even then an uncertain evolutionary correction remains.

In a recent study of high-redshift ($1 \leq z \leq 2.2$) quasi-stellar objects with the *IUE* satellite, Bechtold *et al.* (1984) find a general steepening of spectral energy distributions shortward of ~ 1200 Å. The amount of observed steepening increases with increasing redshift, but it is uncorrelated with the QSO luminosity, which, according to these authors, arises from absorption by intervening material along the line of sight.

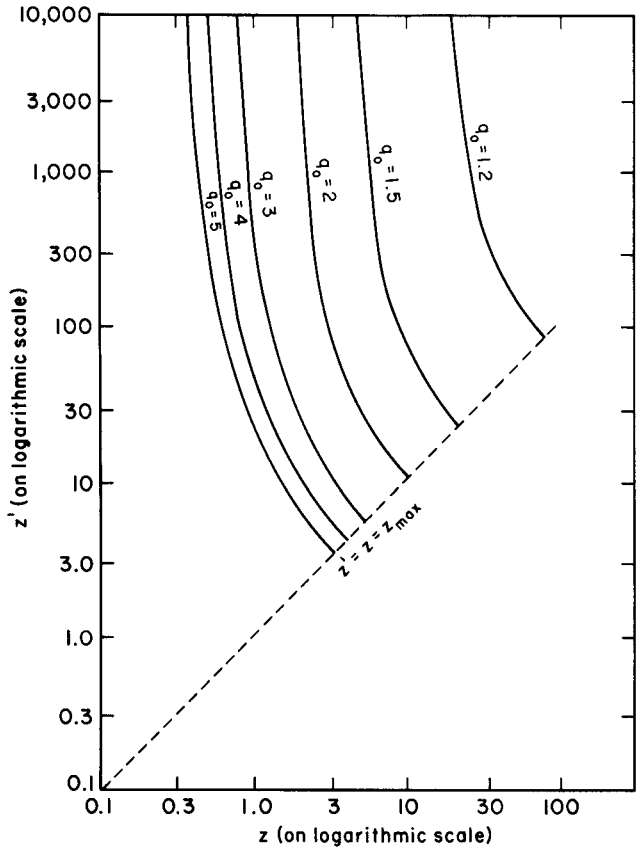

FIG. 2.—The plot of z' against z for $q_0 = 1.2, 1.5, 2, 3, 4, 5$. The dotted line represents the line of maximum redshifts z, below which two images are seen. The vertical asymptotes to the curves correspond to $z_{min}(q_0)$, the redshift which must be exceeded for the counterimage to be visible.

If gas in intervening objects causes absorption, then a useful guide is the number of intervening objects out to redshift z. Following Burbidge *et al.* (1977) this number is

$$\mu(z) = \frac{c}{H_0 l_0} f(z) \; ; \qquad f(z) \equiv \frac{1}{3q_0{}^2} \{[q_0 z - (1 - 3q_0)](1 + 2q_0 z)^{1/2} + (1 - 3q_0)\} \; . \tag{29}$$

Here l_0 is the mean free path for interception of light by the intervening objects. Table 1 indicates how $f(z)$ increases with z but decreases with q_0. If we take $H_0 = 50$ km s^{-1} Mpc^{-1} and l_0 = the value used by Burbidge *et al.* (1977) for disk galaxies, then $c/H_0 l_0 \approx 1/40$ and $\mu(z)$ is less than ~ 1 for all entries of Table 1. However, if one replaces disk galaxies by extensive halos, the value of $\mu(z)$ goes up by a factor ~ 40, and the effect of absorption becomes very significant.

Another possible contributer to en route absorption might be intergalactic dust. For example, Chitre and Narlikar (1976) have shown that long whispers of graphite with a total density of $\sim 10^{-33}$ g cm^{-3} can produce significant absorption en route, even for modest redshifts. For example, for the $q_0 = 1$ model the absorption increases the apparent magnitude by 0.87, at $z = 1$. For $q_0 = 5$ the same formula produces at $z = 5$ a magnitude increase of 13.87. Again, these estimates depend upon the highly uncertain knowledge of intergalactic dust.

TABLE 1

EXPECTED NUMBER[a] OF INTERVENING GALAXIES OUT TO REDSHIFT z IN FRIEDMANN MODELS OF GIVEN q_0

	q_0		
REDSHIFT z	1	3	5
1	1.065	0.782	0.653
3	3.743	2.448	1.966
5	7.072	4.447	3.527
10	17.663	10.696	8.389
20	46.289	27.407	21.363

[a] To get the expected number multiply the entries in the above table by $c/H_0 l_0$.

It is likely that young galaxies with very bright stars were considerably more luminous at the epochs when light rays forming their counterimages left for the observer, than at the more recent epochs of the direct image formation. In such circumstances luminosity evolution would help the detection of counterimages.

Not taking into account these uncertainties from (i)–(iii), we may compute the apparent bolometric magnitude difference between the two images according to the formula

$$\Delta m(z) = 5 \log \frac{D(z')}{D(z)}, \tag{30}$$

where $D(z)$ is the luminosity distance at redshift z in the given Friedmann model (cf. for example, Narlikar 1983). Δm denotes the extent by which the counterimage is *fainter* than the direct image of redshift z. A simple calculation gives

$$\Delta m(z) = 5 \log \frac{1+z'}{1+z} = -5 \log \frac{1+\cos(2\psi_0 - \psi_e)}{1-\cos\psi_e}. \tag{31}$$

(The formula is simplified because both images are at the same radial-r coordinate with respect to the observer.)

Figure 3 gives a plot of $\Delta m(z)$ against z for a range of values of q_0. For $q_0 = 3$, the value of Δm at $z = 2$ is ~ 4.3 mag. Thus a quasi-stellar object of redshift z and apparent magnitude, say, 19 mag, will have a counterimage at ~ 23.3 mag. This illustrates the fact that unless the factors (i)–(iii) intervene, the counterimages are not too faint to detect by modern technology.

c) *Redshift Cutoff*

Figure 4 describes the spacetime diagram in a schematic fashion, where the time axis is vertically upward and the horizontal axis gives the χ-coordinate. The antipodal points appear on the opposite sides of the t-axis and have values χ and $\pi - \chi$, respectively. For convenience we have shown the world lines a, b of two QSOs on the left-hand side of the t-axis by continuous lines and their antipodal lines at a', b' by broken lines on the right-hand side of the t-axis. The world line a has $\chi \equiv \chi_a < \pi/2$, while b has $\chi \equiv \chi_b > \pi/2$.

In the spherical universe the antipodes are not identified, and the QSO b will be seen further than QSO a. However, in the elliptical universe the antipodes are identified. Thus b will also be seen at b'. The observer will find it easier to locate b' (at lower redshift) than b. Since all the near images tend to be with redshifts $\leq z_{max}$ given by equation (26), the above selection effect may operate to place an upper limit on the redshifts that can be easily measured. For example, for $q_0 = 4.25$, $z_{max} \approx 4$. This could very well be the cause of the redshift cutoff at $z \approx 4$ seen in the QSO population.

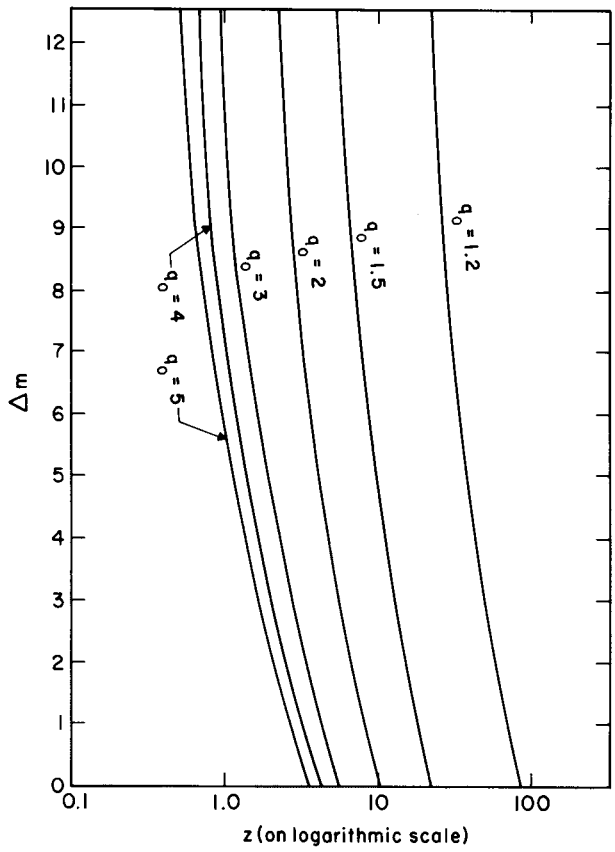

FIG. 3.—The difference in the apparent bolometric magnitudes of the counterimage and the direct image plotted against the redshift of the latter in models with $q_0 = 1.2, 1.5, 2, 3, 4, 5$.

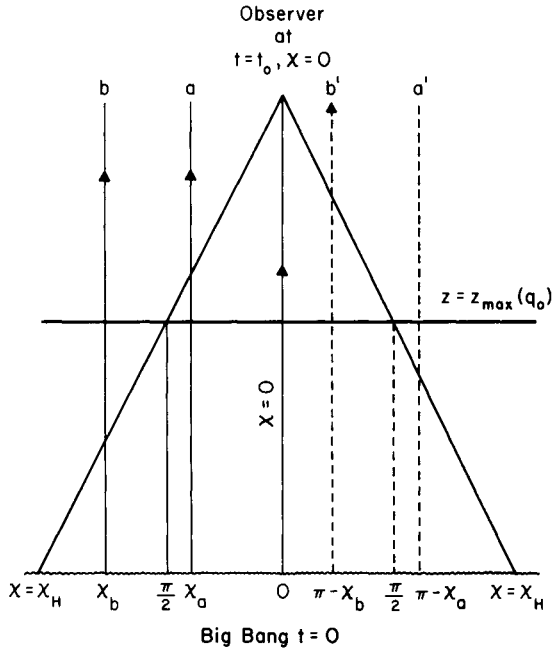

FIG. 4.—The spacetime diagram in which the vertical direction denotes cosmic time t and the horizontal displacement from the central vertical line the radial coordinate χ. The present observer is at $t = t_0$, $x = \chi_0$. The past light cone from the observer intersects the $t = 0$ (big bang) hypersurface at $\chi = \chi_H$, denoting the particle horizon.

IV. CONCLUSION

Connectivity, like differential geometry, is an important property of spacetime. Currently favored cosmological models suggest that the large-scale structure of the universe does not conform to Euclidean geometry, although that geometry is consistent with purely local observations. Likewise, one may ask whether the large-scale connectivity of the universe does conform with the simple ideas based on our local region. The elliptical model has a different connectivity, and its effects are detectable by studies of the distant parts of the universe.

The observational effects discussed here become important only for $q_0 > 1$. These models suffer from one drawback: even for $H_0 = 50$ km s^{-1} Mpc^{-1}, the age of the universe for q_0 in the range 3–5 is as low as 7–8 billion years. Is this age too low to accommodate the ages of galaxies, globular clusters, etc.? In this context it is worth mentioning that if Hubble's constant is 100 km s^{-1} Mpc^{-1}, the age of the $q_0 = \frac{1}{2}$ (marginally open) Friedman model favored by the inflationary scenarios is lower than 7 billion years. That such low age models are tolerated is a reflection of the present-day uncertainty surrounding the age determination of astronomical systems, including the universe. Against this background a deceleration parameter as high as above might still be acceptable.

With the rapid progress in the observational studies of faint objects, the tests proposed here could be further sharpened and used to decide the important question whether the large-scale connectivity of the universe is more unusual than indicated by local observations.

We thank Richard Green, Jay Gallagher, and Geoffrey Burbidge for discussions and comments. One of us (J. V. N.) gratefully acknowledges the hospitality of the Kitt Peak National Observatory.

REFERENCES

Bechtold, J., Green, R. F., Weymann, R. J., Schmidt, M., Estabrook, F. B., Sherman, R. D., Wahlquist, H. D., and Heckman, T. M. 1984, *Ap. J.*, **281**, 76.
Burbidge, G., O'Dell, S. L., Roberts, D. H., and Smith, H. E. 1977, *Ap. J.*, **218**, 33.
Chitre, S. M., and Narlikar, J. V. 1976, *Ap. Space Sci.*, **44**, 101.
Eddington, A. S. 1923, *The Mathematical Theory of Relativity* (Cambridge: The University Press), p. 157–158.
Narlikar, J. V. 1983, *Introduction to Cosmology* (Boston: Jones and Bartlett).
Petrosian, V., Salpeter, E. E., and Szekeres, P. 1967, *Ap. J.*, **147**, 1222.

J. V. NARLIKAR and T. R. SESHADRI: Theoretical Astrophysics Group, Tata Institute of Fundamental Research, Homi Bhabha Road, Bombay 400 005, India